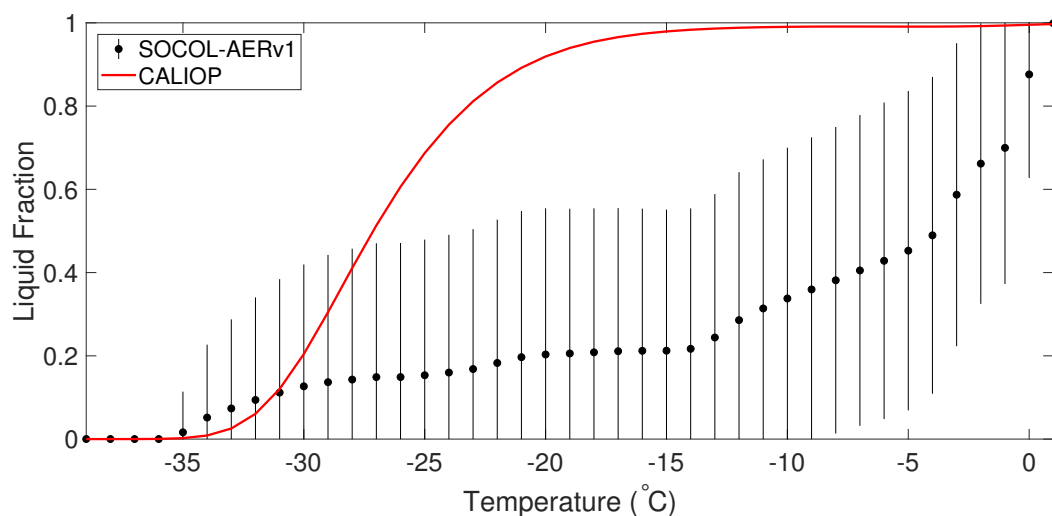


# Improved tropospheric and stratospheric sulfur cycle in the aerosol-chemistry-climate model SOCOL-AERv2

## Supplementary Material

Aryeh Feinberg, Timofei Sukhodolov, Bei-Ping Luo, Eugene Rozanov, Lenny H.

E. Winkel, Thomas Peter, Andrea Stenke



**Figure S1:** The liquid fraction of clouds in the mixed-phase cloud regime ( $-38\text{ }^{\circ}\text{C} < T < 0\text{ }^{\circ}\text{C}$ ) simulated by SOCOL-AERv1 based on ECHAM5 during a one-year simulation (solid circles). 12-hourly model output in all grid boxes with clouds is averaged in 1 degree temperature bins, with standard deviation bars included. The red curve shows the fitted sigmoid function (Hu et al., 2010) for the supercooled liquid fraction,  $\text{SLF}_{\text{Hu}}$ , derived from CALIOP Lidar measurements on board of the CALIPSO satellite. In its aqueous chemistry scheme, SOCOL-AERv2 adopts the satellite SLF to calculate the liquid water content from the model's total water content,  $\text{LWC} = \text{SLF}_{\text{Hu}} \times \text{TWC}$ .

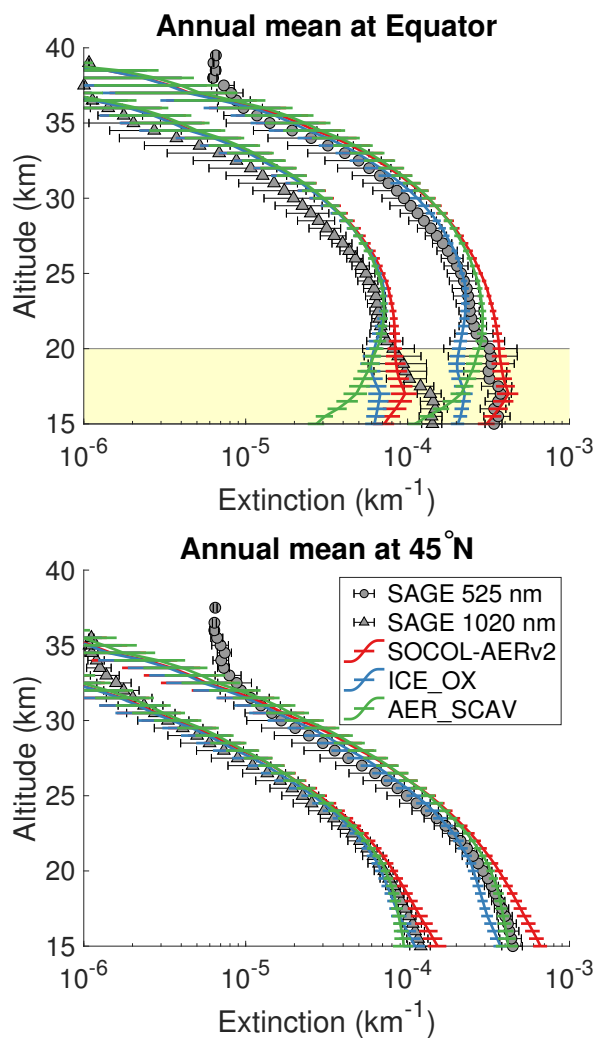


**Figure S2:** Comparison between annual mean model extinctions at 525 and 1020 nm and SAGE II measurements from the GloSSAC project (Thomason et al., 2018) at the Equator (*top*) and 45° N (*bottom*). Observations are averaged between 2000–2004, representing the volcanically quiescent part of the record. Model results are averaged over 5 years of the year 2000 time-slice for SOCOL-AERv2, ICE\_OX, and AER\_SCAV. Horizontal bars represent the modelled or observed standard deviation. The highlighted region in the upper plot corresponds to the altitudes where non-sulfate aerosols may play a role.

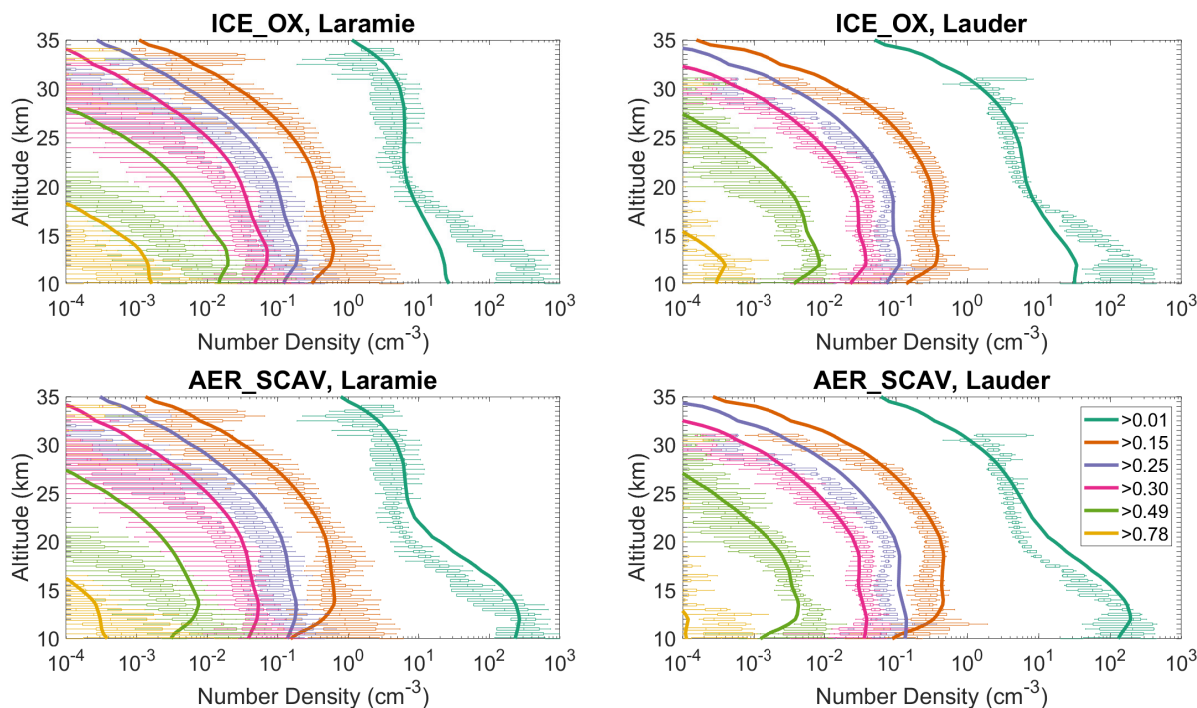


**Figure S3:** Number densities of particle size bins measured by OPC (Deshler et al., 2003; Deshler, 2008) and modelled by ICE\_OX and AER\_SCAV over Laramie, Wyoming, USA (41° N, 105° W) and Lauder, New Zealand (45° S, 170° W). Measured number densities are shown as box plots (minimum excluding outliers below the 0.4 percentile, 25<sup>th</sup> percentile, median, 75<sup>th</sup> percentile, maximum excluding outliers above the 99.6 percentile) and modelled number densities as solid lines. For the Laramie plots (*left*), OPC measurements are used from the period 1999–2008 and zonal mean model results are averaged over the 5 years of the time-slice. For the Lauder plots (*right*), OPC measurements are used from January to April 1998–2001 and zonal mean model results are averaged from January to April over 5 years of the time-slice. Model results are weighted with the counting efficiencies for OPC channels from Deshler et al. (2019) for direct comparability with the measurements.

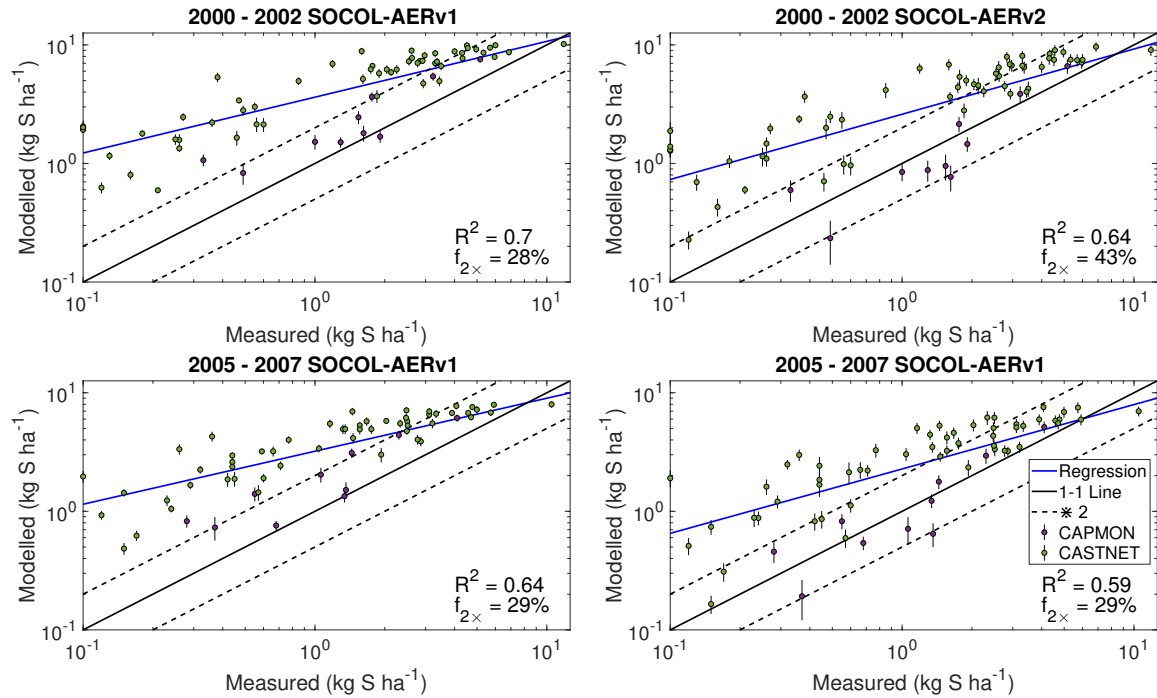


**Figure S4:** Evaluation of modelled  $\text{SO}_2$  dry deposition against North American measurement sites from the WMO database (Vet et al., 2014). SOCOL-AERv1 and SOCOL-AERv2 are compared with measurements in two different time periods, 2000–2002 and 2005–2007. The ensemble standard deviation for the model results is shown as vertical bars. A power regression between the simulation results and measurements is shown in blue, and can be compared to the one-to-one line shown in black. Two model evaluation metrics are listed on the plots: the goodness of fit of the power regression between model and measurements ( $R^2$ ) and the fraction of sites for which the model is within a factor of 2 of measurements ( $f_{2\times}$ ). Points are colored according to the measurement network of the sites.

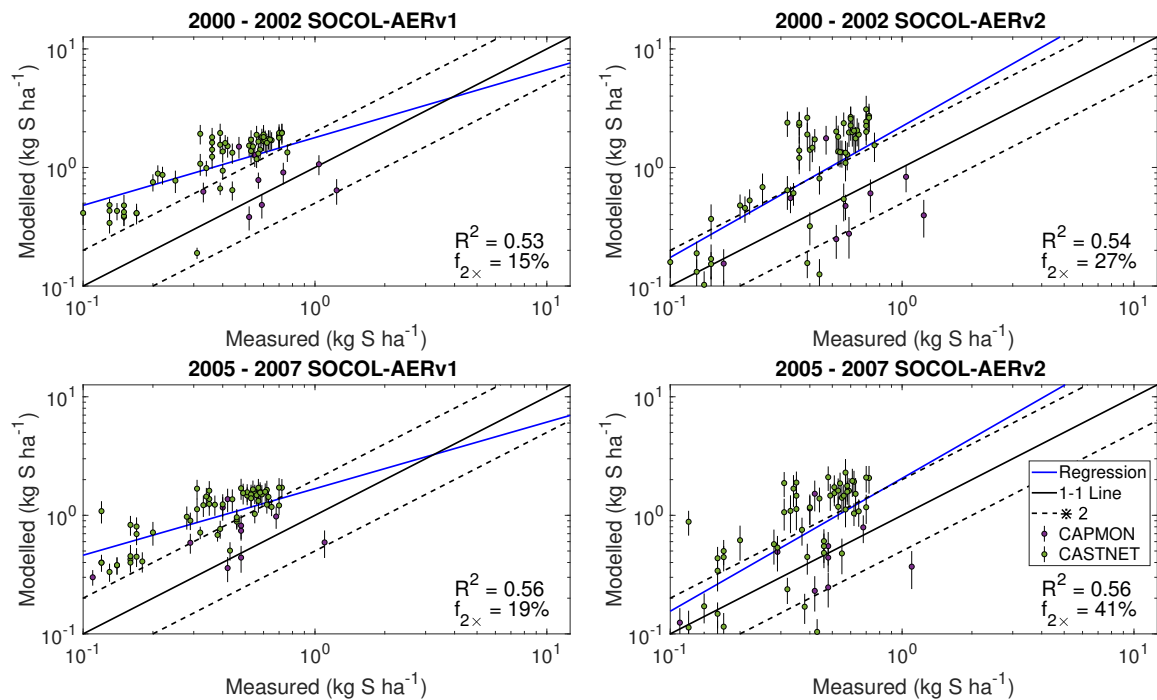


**Figure S5:** Evaluation of modelled sulfate aerosol dry deposition against North American measurement sites from the WMO database (Vet et al., 2014). SOCOL-AERv1 and SOCOL-AERv2 are compared with measurements in two different time periods, 2000–2002 and 2005–2007. The ensemble standard deviation for the model results is shown as vertical bars. A power regression between the simulation results and measurements is shown in blue, and can be compared to the one-to-one line shown in black. Two model evaluation metrics are listed on the plots: the goodness of fit of the power regression between model and measurements ( $R^2$ ) and the fraction of sites for which the model is within a factor of 2 of measurements ( $f_{2\times}$ ). Points are colored according to the measurement network of the sites.

**Table S1:** The time periods covered by model intercomparison projects of sulfur deposition and this study.

| Project Name | Simulation Period | Observation Period | Reference              |
|--------------|-------------------|--------------------|------------------------|
| Photocomp    | 2000              | 2000               | Dentener et al. (2006) |
| ACCMIP       | 2000              | 2000–2002          | Lamarque et al. (2013) |
| HTAP I       | 2001              | 2000–2002          | Vet et al. (2014)      |
| HTAP II      | 2010              | 2009–2011          | Tan et al. (2018)      |
| SOCOL-AERv2  | 2000–2002         | 2000–2002          | This study             |
|              | 2000–2002         | 2005–2007          |                        |

## S1 References

- Dentener, F., Drevet, J., Lamarque, J.-F., Bey, I., Eickhout, B., Fiore, A. M., Hauglustaine, D., Horowitz, L. W., Krol, M., and Kulshrestha, U.: Nitrogen and sulfur deposition on regional and global scales: A multimodel evaluation, *Global biogeochemical cycles*, 20, 2006.
- Deshler, T.: A review of global stratospheric aerosol: Measurements, importance, life cycle, and local stratospheric aerosol, *Atmospheric Research*, 90, 223–232, 2008.
- Deshler, T., Hervig, M., Hofmann, D., Rosen, J., and Liley, J.: Thirty years of in situ stratospheric aerosol size distribution measurements from Laramie, Wyoming (41 N), using balloonborne instruments, *Journal of Geophysical Research: Atmospheres*, 108, 2003.
- Deshler, T., Luo, B., Kovilakam, M., Peter, T., and Kalnajs, L. E.: Retrieval of aerosol size distributions from in situ particle counter measurements: instrument counting efficiency and comparisons with satellite measurements, *Journal of Geophysical Research: Atmospheres*, 2019.
- Hu, Y., Rodier, S., Xu, K., Sun, W., Huang, J., Lin, B., Zhai, P., and Josset, D.: Occurrence, liquid water content, and fraction of supercooled water clouds from combined CALIOP/IIR/MODIS measurements, *Journal of Geophysical Research: Atmospheres*, 115, 2010.
- Lamarque, J.-F., Dentener, F., McConnell, J., Ro, C.-U., Shaw, M., Vet, R., Bergmann, D., Cameron-Smith, P., Doherty, R., and Faluvegi, G.: Multi-model mean nitrogen and sulfur deposition from the Atmospheric Chemistry and Climate Model Intercomparison Project (ACCMIP): evaluation historical and projected changes, 2013.
- Tan, J., Fu, J. S., Dentener, F., Sun, J., Emmons, L., Tilmes, S., Sudo, K., Flemming, J., Jonson, J. E., and Gravel, S.: Multi-model study of HTAP II on sulfur and nitrogen deposition, *Atmospheric Chemistry and Physics*, 18, 6847–6866, 2018.
- Thomason, L. W., Ernest, N., Milln, L., Rieger, L., Bourassa, A., Vernier, J.-P., Manney, G., Luo,

B., Arfeuille, F., and Peter, T.: A global space-based stratospheric aerosol climatology: 1979-2016, *Earth System Science Data*, 10, 469–492, 2018.

Vet, R., Artz, R. S., Carou, S., Shaw, M., Ro, C.-U., Aas, W., Baker, A., Bowersox, V. C., Dentener, F., and Galy-Lacaux, C.: A global assessment of precipitation chemistry and deposition of sulfur, nitrogen, sea salt, base cations, organic acids, acidity and pH, and phosphorus, *Atmospheric Environment*, 93, 3–100, 2014.